hydrology

Article

Vulnerability to Aquifer Pollution in the Mexican Wine Producing Valley of Guadalupe, México

Guadalupe Díaz-Gutiérrez [1], Luis Walter Daesslé [2,*], Francisco José Del-Toro-Guerrero [1,2], Mariana Villada-Canela [1] and Georges Seingier [3]

[1] Instituto de Investigaciones Oceanológicas, Universidad Autónoma de Baja California, Carr. Transpeninsular 3917, Ensenada 22860, Baja California, Mexico; diazg9@uabc.edu.mx (G.D.-G.); francisco.deltoro@uabc.edu.mx (F.J.D.-T.-G.); mvilladac@uabc.edu.mx (M.V.-C.)
[2] Instituto de Ingeniería, Calle de la Normal, Insurgentes Este, Mexicali 21280, Baja California, Mexico
[3] Facultad de Ciencias Marinas, Universidad Autónoma de Baja California, Carr. Transpeninsular 3917, Ensenada 22860, Baja California, Mexico; georges@uabc.edu.mx
* Correspondence: walter@uabc.edu.mx; Tel.: +52-646-1528222

Abstract: Groundwater pollution is one of the main challenges in our society, especially in semi-arid Mediterranean regions. This issue becomes especially critical in predominantly agricultural areas that lack comprehensive knowledge about the characteristics and functioning of their aquifer system. Vulnerability to groundwater pollution is defined as the sensitivity of the aquifer to being adversely affected by an imposed pollution load. For the Guadalupe aquifer, various indicators including water level depth, level variation, aquifer properties, soil composition, topography, impact on the vadose zone, and hydraulic conductivity were evaluated to establish spatial vulnerability categories ranging from very low to very high. Two pollution vulnerability scenarios (wet and dry) were studied. The results were compared with the analysis of nitrate concentration and distribution (2001, 2020, and 2021) from samples collected in the field. In the Calafia area, which predominantly relies on viticulture, the primary recharge inputs were identified in areas with a high vulnerability to pollution. Surprisingly, these vulnerable areas exhibited lower nitrate concentrations. This scenario underscores the need for effective management measures to safeguard aquifers in agricultural regions.

Keywords: vulnerability assessment; aquifer; nitrate; GIS; DRASTIC; geostatistics; groundwater management

check for updates

Citation: Díaz-Gutiérrez, G.; Daesslé, L.W.; Del-Toro-Guerrero, F.J.; Villada-Canela, M.; Seingier, G. Vulnerability to Aquifer Pollution in the Mexican Wine Producing Valley of Guadalupe, México. *Hydrology* **2024**, *11*, 16. https://doi.org/10.3390/hydrology11020016

Academic Editor: Peiyue Li

Received: 8 November 2023
Revised: 3 December 2023
Accepted: 7 December 2023
Published: 31 January 2024

Copyright: © 2024 by the authors. Licensee MDPI, Basel, Switzerland. This article is an open access article distributed under the terms and conditions of the Creative Commons Attribution (CC BY) license (https://creativecommons.org/licenses/by/4.0/).

1. Introduction

The forward-looking management and protection of groundwater resources and their protection from pollution represents a significant challenge for our society [1]. In developing countries, the rapid growth of population triggers urban expansion and the intensification of agricultural practices, posing a substantial risk of water resource pollution [2]. The quality and availability of water are inherently shaped by geographical, geological, and climatological characteristics, consequently creating conditions of scarcity or abundance of this vital resource [3]. Inadequate management of water resources, such as intensive groundwater extraction, can surpass the natural recharge capacity in arid and semi-arid areas [4], leading to the overexploitation of aquifers [5].

Aquifers are hydrogeological units that exhibit high vulnerability to pollution [6]. The chemical composition of groundwater can be influenced by both natural or anthropogenic factors [7]. Natural factors encompass climate, interactions, and the residence time of groundwater within the geological environment (dissolution of salts or minerals during its flow). Anthropogenic factors directly stem from human activities, such as the use of agrochemicals in agriculture (including fertilizers, herbicides, and pesticides) [8]. Agricultural irrigation exerts significant pressure, potentially leading to salinization and, in some cases, groundwater pollution when irrigation water has poor quality [9].

The quantity and quality of water are contingent upon land use in the areas responsible for capturing, conveying, storing, supplying, and replenishing the water resource [10]. Water quality is primarily determined by the presence of dissolved or suspended materials, substances, and organisms within it [11]. Water quality is not an absolute criterion; it can be deemed adequate or inadequate depending on its intended use [12]. Therefore, it is necessary to understand certain chemical characteristics that influence its quality and potential applications. These include parameters such as dissolved oxygen, suspended particles, dissolved salts, and the presence and concentration of toxic compounds, bacteria, and other microorganisms. Consequently, comprehending the potential and behavior of key pollutants from their source to the point of groundwater contact, along with understanding the characteristics of the aquifer system, becomes imperative [13].

There are several standardized methods available to assess the vulnerability of aquifers to pollution. Intrinsic vulnerability to pollution considers the physical properties of the aquifer system (e.g., inherent geological, hydrological, and hydrogeological characteristics) [14]. It is defined as the sensitivity of the aquifer to be adversely affected by an imposed pollutant load [15]. On the other hand, specific vulnerability is defined as the vulnerability of groundwater to particular pollutants, considering their properties, i.e., physical and biogeochemical attenuation processes (e.g., nitrate concentration) [16]. Indirect methods used to estimate the spatial vulnerability to pollution of an aquifer rely on indices, statistics, and geological processes [17,18]. The most widely adopted method worldwide is DRASTIC [19,20], which assesses vulnerability using seven parameters: depth to groundwater (D), net recharge (R), aquifer medium (A), soil (S), topography (slope T), vadose zone impact (I), and hydraulic conductivity (C). Each parameter has classes with a ranking value and weight based on the importance of its characteristics, which can indicate varying levels of vulnerability to aquifer pollution. These indirect methods consider the characteristics of the aquifer environment and incorporate factors related to the characteristics of contaminant transport through unsaturated and saturated zones (e.g., morphological, hydrological, edaphological, hydraulic conductivity, water table) [14].

In different countries, research has validated and modified the intrinsic vulnerability methods (DRASTIC) [21]. For example, [22] assessed the vulnerability of an alluvial aquifer in a semi-arid environment in Algeria, where they determined zones from very low to very high vulnerability, mainly due to the urbanization of the area. They reclassified values in only three classes, to adopt protection measures in the most vulnerable area, and to have a tool for planning and water management [23]. In China [24], the DRASTIC method was applied as a nitrate pollution prevention tool, where they optimized the parameters by replacing them with quantitative information on aquifer thickness, nitrate attenuation intensity, hydraulic resistance, and groundwater velocity, and obtained improved results with a more uniform distribution of vulnerability classes in correlation to nitrate concentration, in order to formulate groundwater protection plans [25,26] and estimate specific vulnerabilities such as the risk of nitrate pollution [27,28]. In southern Mexico, ref. [29] using DRASTIC and comparing with the spatial distribution of nitrate concentration, researchers showed that there was no relationship between nitrate and vulnerability at the site, recommending that more specific vulnerability methodologies had to be applied.

Indirect methods are sometimes complemented with site-measured hydrochemical data to analyze and validate the specific vulnerability of groundwater to a pollutant, depending on the level of accessibility of the information and the degree of analysis of the investigation [30]. Aquifer vulnerability assessment studies classify zones from negligible to very high pollution vulnerability, including sensitivity analysis and multivariate statistical tests [13,31]. Higher vulnerability zones indicate a higher susceptibility to pollution and pollutant infiltration that will negatively affect the aquifer. The outcomes produce aquifer vulnerability maps validated with the concentration of nitrates. The spatial distribution of nitrates reveals areas with high and low levels, which are subsequently correlated with moderate, high, and very high vulnerability zones, respectively [32].

Nitrates are naturally present in diverse ecosystems. Their presence in groundwater is mainly associated with sediment consolidation processes and anthropogenic activities such as agriculture and livestock farming [33,34]. The Mexican Official Standard NOM-127-SSAI-2021 states that the maximum permissible levels of nitrate nitrogen in water for human consumption are 11 mg L^{-1}, or its equivalence to nitrates of 48.62 mg L^{-1} [35]. Exceeding the permissible concentration limit can have severe and long-term detrimental effects on human health (e.g., methemoglobinemia in infants, congenital disabilities, health effects in adults such as stomach and liver damage, and can lead to cancer), depending on the exposure time [36–39]. Consequently, it is crucial to monitor concentration levels closely to prevent the consumption of contaminated water or, ideally, to take remedial measures at high concentration levels. Assessing the vulnerability of an aquifer to pollution is essential to develop strategies for management, remediation, and preventive actions in groundwater use.

Our study site in northwestern Mexico is the wine-producing Guadalupe Valley (GV). Here, the Guadalupe aquifer (GA) serves as the primary water source for the GV agricultural region and its surrounding areas. The GV is under tremendous pressure from land use change and emerging tourism, which generates a high demand for water resources and changes in its ecosystem balance. The (GA) has a contribution to natural recharge by surface runoff of ca. 40% [40] and approximately 10% of the volume of water used for agricultural irrigation returns to the aquifer through percolation [41]. These return flows from irrigation may significantly contribute to pollution of the aquifer, specially by fertilizers like nitrate, which is highly mobile in solution. Therefore, the objective of this study is to use the DRASTIC method to identify areas within the GA that are particularly vulnerable to pollution. The analysis considered two temporal scenarios spanning the period 2008 to 2017. The first scenario represented a period of higher rainfall (April 2011), while the second scenario represented a period of lower rainfall (December 2016). These periods were selected as they corresponded to the highest and lowest water availability in the GA, respectively, as indicated by the depth of groundwater. In the first scenario, the groundwater level approaches the natural ground level, while in the second scenario, there is a lower saturated zone thickness. By comparing these two scenarios it was possible to identify spatial variations in the vulnerability of the GA. Such analysis was accomplished by integrating the parameters of the DRASTIC method and the results were assessed in terms of the spatial concentration of nitrate in the aquifer.

2. Materials and Methods

2.1. Study Area

The GA is located 18 km north of Ensenada in the northwestern region of Baja California, Mexico (Figure 1), between parallels 32°0′ and 32°8′ N latitude and meridians 116°28′ and 116°45′ W longitude, 115 km south of the USA border. It is a geologic formation in an intermontane valley (GV) close to the Pacific Ocean, covering an area of ~80 km^2 [42].

Geologically, the GA is an unconfined heterogeneous aquifer formed by two tectonic grabens, which resulted from normal faults, filled by unconsolidated Quaternary sediments (gravels, sands, clay lenses, and silts) [43]. The geology and geomorphology are described in [44]. The Calafia graben (located in northeast GV) has a maximum depth of 350 m, and the Porvenir graben (located in southwest GV) reaches a maximum depth of 100 m [11]. In total, the potential storage capacity of the GA is ~340 hm^3 [45]. Surface runoff, seepage from ephemeral Arroyo Guadalupe runoff, is the primary main source of GA's recharge, followed by vertical recharge associated with faults and fractures on the flanks of the valley, and percolation of agricultural irrigation [46]. Previous studies mention that recharge occurs mainly in the winter season, with events more significant than 50 mm/month, indicating that soil depth and lack of vegetation cover play a critical role in recharge. GA has a total recharge of 18.8 $hm^3\ yr^{-1}$ [42]. Land use in GV is mainly agricultural [40]. Vine and olive crops are the most representative and suitable for development in the semi-arid Mediterranean climate of the region [47].

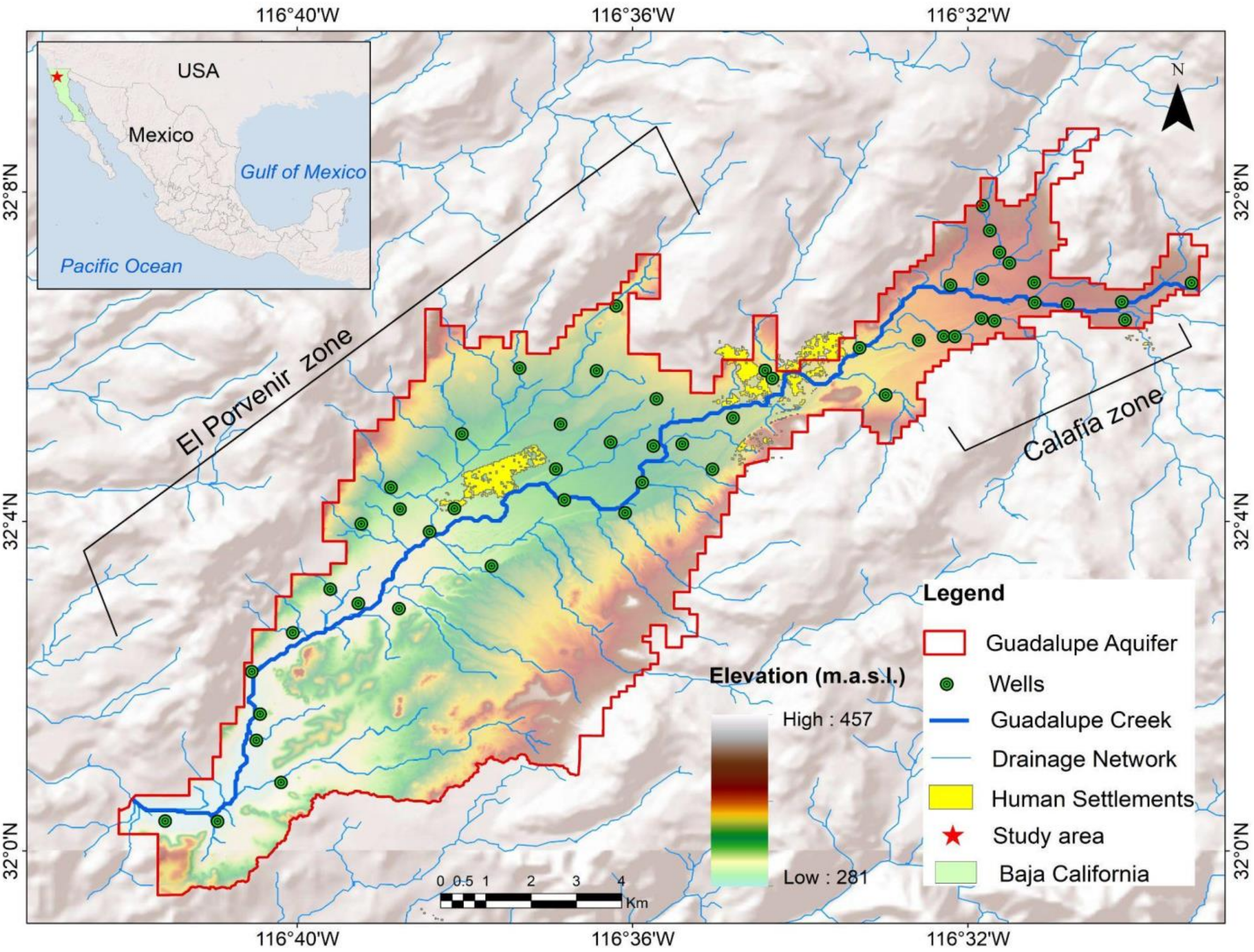

Figure 1. Location of the study area and well samples for nitrate concentrations in three different years (2001, 2020, and 2021).

Four hydrological seasons have been identified in the region: a winter wet season (WS; January–March), a dry season (DS; June–September), and two transitional seasons of WS-DS (April–May) and DS-WS (October–November) [48]. Mean annual precipitation is 298 mm, and most precipitation events occur during WS, with some sporadic precipitation events the rest of the year. Historically, the main interannual precipitation contribution originates during WS (77%), with February and January being the wettest months. The DS season contributes only 2% of the precipitation, and the remaining 21% occurs in the transitional seasons. The mean annual temperature is ~17.9 °C, and the WS temperature is ~13.4 °C, during DS it is ~23.1 °C, and in the transition months it ranges between ~15–20 °C. Historically, August has been the warmest month, with an average of 24.7 °C. The only source of recharge of the GA is precipitation and in turn, the GA is the only direct source of water supply to meet the region's water demands. The average annual recharge is 18.8 $hm^3 yr^{-1}$ (calculated from 2010 to 2013), and the volume of groundwater extraction amounts to 37.1 $hm^3 yr^{-1}$, generating a deficit of -18.4 $hm^3 yr^{-1}$ [42] as it is an overexploited aquifer.

2.2. DRASTIC Method

The DRASTIC method employs a numerical ranking system, assigning relative weights to assess an aquifer's intrinsic vulnerability to pollution [19]. This method was developed by the United States Environmental Protection Agency (USEPA). The method traditionally considers and weighs seven parameters in assessing vulnerability to groundwater pollution (Table 1).

Table 1. Description of the DRASTIC method parameters (modified from [19]).

Parameter	Description
D (Depth to Water Table)	The depth to water table indicates the thickness of the unsaturated zone, which is the length through which water travels by infiltration transporting the pollutant until it reaches the saturated zone of the aquifer [49]. The saturated zone is dynamic in unconfined aquifers, fluctuating with the seasons, extractions, and water availability. The deeper the groundwater level, the greater the probability of natural attenuation.
R (Recharge)	Recharge indicates the amount of water that infiltrates from the soil surface to the water table, increases the saturated thickness, and is the main transport of potential contaminants [18].
A (Aquifer Media)	The aquifer media represents the lithology and structure of consolidated or unconsolidated sediments, in particular, the capacity of the porous and/or fractured medium to retain and transport water. A is considered a potential pathway for contaminant transport depending on its porosity (primary or secondary) [31]. Overall, the larger the size of the sediment or the more fractures it has, the higher the permeability, the lower the contaminant attenuation capacity, and the higher the probability of pollution.
S (Soil)	Soil type represents the uppermost layer of the aquifer, characterized by biological activity and exposure to erosion, where its thickness and texture are significant for attenuation, biodegradation, sorption, and volatilization processes. The S parameter impacts the amount of water that infiltrates into the soil, and its texture modulates the vertical movement of a pollutant to be transported by water through the space between the particles (depending on the size) in the vadose zone [50]. Anthropogenic practices on the land surface such as agricultural applications, can be a potential source of pollution.
T (Topography)	In this context, topography represents the slope and controls of surface and subsurface runoff velocity. In the case of a potential pollutant, the effect may be accumulation; for example, in agricultural areas with a lower slope percentage, nitrate concentration may accumulate due to the intensive use of fertilizers [50].
I (Impact of the Vadose Zone)	The impact on the vadose zone corresponds to the site above the water table, controlling the length and time travel of water towards the saturated zone, thus influencing the available time for pollutant transport attenuation processes [51].
C (Hydraulic Conductivity)	Hydraulic conductivity measures the speed with which water can pass through the porous or fractured medium of the aquifer [31]. Specifically, it measures the movement of water flowing through a porous medium. This parameter is controlled by the amount and interconnectedness of voids within the aquifer as a consequence of intergranular porosity and fracturing.

The application of the DRASTIC method assumes the following: (a) the contaminant is introduced from the soil surface, (b) the contaminant reaches the water table by precipitation/infiltration processes, and (c) the contaminant has the same mobility as water.

2.3. Sampling and Measurements

Two temporal scenarios, one with higher and one with lower water availability (WS and DS), were analyzed to identify the degree of vulnerability of the aquifer to pollution. The parameters of depth to groundwater level (D) and recharge (R) vary in both scenarios, while aquifer media (A), soil (S), topography (T), impact on the vadose zone (I), and hydraulic conductivity (C) parameters are constant in both scenarios.

Hydrogeological, geological, soil texture, and topographical data were used to classify the parameters. Parameters were calculated from databases and thematic maps and transformed in integer value raster format with a 5 m spatial resolution in ArcGIS 10.8 and QGIS 3.24.2 [52,53]. Then, the results were classified following the DRASTIC method to create pollution vulnerability thematic maps.

Parameters

The analysis used groundwater level depth data from 52 wells for the wet scenario (April 2011) and 49 wells for the dry scenario (December 2016). The monitoring wells are distributed along the GA surface, from southwest to northeast (Figure 1).

In this research, for a semi-arid Mediterranean environment, the recharge parameter was represented by the variation in groundwater levels observed in the monitoring wells under both scenarios (April 2010, wet and November 2009, dry). The groundwater level measurements provide insights into the recharge process in the GA.

The aquifer media parameter was derived through georeferencing the "Francisco Zarco I11-D82" Baja California 1:50,000 geological map [54]. Lithology was digitized and classified based on the geological formation types within the study area.

The soil parameter was obtained during field visits from 31 soil samples (0–15 cm depth) collected systematically along the GV. We calculated the relative sand and silt–clay content in the laboratory (soil and sediment laboratory) following the granulometric analysis method and defined the soil texture. The topography parameter was derived from a 5 m resolution LiDAR Digital INEGI Elevation Model (DEM) and the slope calculation in QGIS 3.24.2. We define the impact on the unsaturated zone parameter from a 1:50,000 geology map from the Mexican Geological Service (SGM). The hydraulic conductivity parameter was represented following the results of [55]. However, qualitative modifications were applied to the data to identify distinct zones on the aquifer surface, e.g., to differentiate the Calafia zone from the Porvenir zone.

Different interpolation methods (Kriging/Cokriging, Inverse Distance Weighting) were tested, but the "Empirical Bayesian Kriging" proved to be the most accurate to generate the prediction maps of the depth to groundwater and recharge from the monitoring sites (wells) and soil parameter from relative sand content in field sites. A logarithmic transformation and a circular smoothed neighborhood type with a factor of 0.5 were applied.

Cross-validation was applied to the prediction maps resulting from modeling in the ArcGIS 10.8 program. The root means square error (*RMSE*) was calculated to assess the quality of the interpolations [56] as follows:

$$RMSE = \sqrt{\frac{\sum_{i=1}^{n} (Pi - Oi)^2}{n}} \quad (1)$$

where *RMSE* is the root mean squared error, *Pi* is the predicted value, *Oi* is the observed value, and *n* is the sample size.

2.4. Application of the DRASTIC Vulnerability Index (DVI)

To model the DVI of the GA, the weighted indices of each parameter were superimposed using the spatial analysis tool "weighted sum" available in ArcMap, and Equation (2) was applied. The numerical ranking factor (*Rj*) in each parameter varies according to the specific characteristics of the study area. *Rj* is based on the ratio of impact, significance, and potential pollution to an aquifer and is represented by values ranging from 1 (least vulnerable) to 10 (most vulnerable). Each parameter is assigned a relative weight (*Wj*) to calculate the DRASTIC vulnerability index (*DVI*), whose values range from 1 (least significant) to 5 (most significant), as shown in Table 2 [19].

The following equation calculates the *DVI* using map algebra in ArcGis 10.8 (for all parameters).

$$DVI = \sum_{j=1}^{7} (Wj * Rj) \quad (2)$$

Typically, the DRASTIC results range from 23 (minimum) to 230 (maximum) (Table 3) [19].

Table 2. Weighting parameter and relative weight of the DRASTIC vulnerability index.

Parameter	DRASTIC Weight
D	5
R	4
A	3
S	2
T	1
I	5
C	3

Table 3. Aquifer pollution vulnerability classes according to the DRASTIC method, following the World Bank Guide to Methodological Proposals for Groundwater Protection [14].

Class	Rating	Definition
Very low	23–64	Presence of confining layers where vertical flow (percolation) is negligible.
Low	65–105	Vulnerable only to conservative pollutants (not commonly affected by chemical reactions in natural processes) when discharged or leached continuously over long periods.
Moderate	106–146	Vulnerable to some contaminants only when continuously discharged or leached.
High	147–187	Vulnerable to many pollutants (except those that are strongly absorbed or easily transformed) in numerous pollution scenarios.
Very high	188–230	Vulnerable to most pollutants with rapid impact in many pollution scenarios.

2.5. Nitrate Analysis NO_3^-

Groundwater samples were collected from 27 wells in 2001, 33 in 2020, and 28 in 2021. Water samples were filtered with 0.45-micron filters, collected in polyethylene bottles, and stored at 4 °C until anion concentration analysis was carried out using the Ion Chromatography System-Dionex Aquion (Thermo Scientific) with the software tool Chromeleon Console 7.2.9, by ion chromatography with chemical suppression [57].

Concentration of nitrate NO_3^- was analyzed with Geographic Information Systems for the graphic representation and construction of spatial distribution maps and temporal behavior.

Finally, the independent parameter of nitrates was validated as a potential pollution factor in the aquifer, depending on the concentrations in the study area, giving a high and very high vulnerability assessment to data exceeding the permissible limits (11 mg L^{-1}) for human consumption of the Mexican Official Standard NOM-127-SSA1-2021 [35]. Grain size analyses of 29 soil samples was carried out by means of a laser particle distribution analyzer HORIBA LA910.

The samples collected in the field and processed in the laboratory were helpful for the optimization of the research, which aims to obtain a point spatial distribution and concentration in the GA.

3. Results and Discussion

The study's findings present two distinct hydrological scenarios (wet and dry) characterized by differences in groundwater depth and groundwater level. The groundwater depth in the wet scenario ranges from 0.8 to 33.9 m (Figure 2a) and in the dry scenario, groundwater depth varies from 4.4 to 57.3 m (Figure 2b). The groundwater level variation is influenced by various factors such as precipitation, surface runoff, and irrigation water return. The groundwater level variation in the wet scenario ranges from 0.7 to 30.0 m

(Figure 2c) and in the dry scenario, from 0 to 5.0 m (Figure 2d). The results of the granulometric analysis revealed that the study site is dominated by sandy soils up to a depth of 30 cm. Approximately 76% of the surface has medium sands and 24% coarse sands located in the El Porvenir zone (Figure 2e). According to Kurczyn-Robledo [58], flat slopes slow down the runoff in the study area. The flat slopes range from 0 to 6% (Figure 2f) and cover 66% of the area, leading to infiltration and possible pollutants transport toward the aquifer.

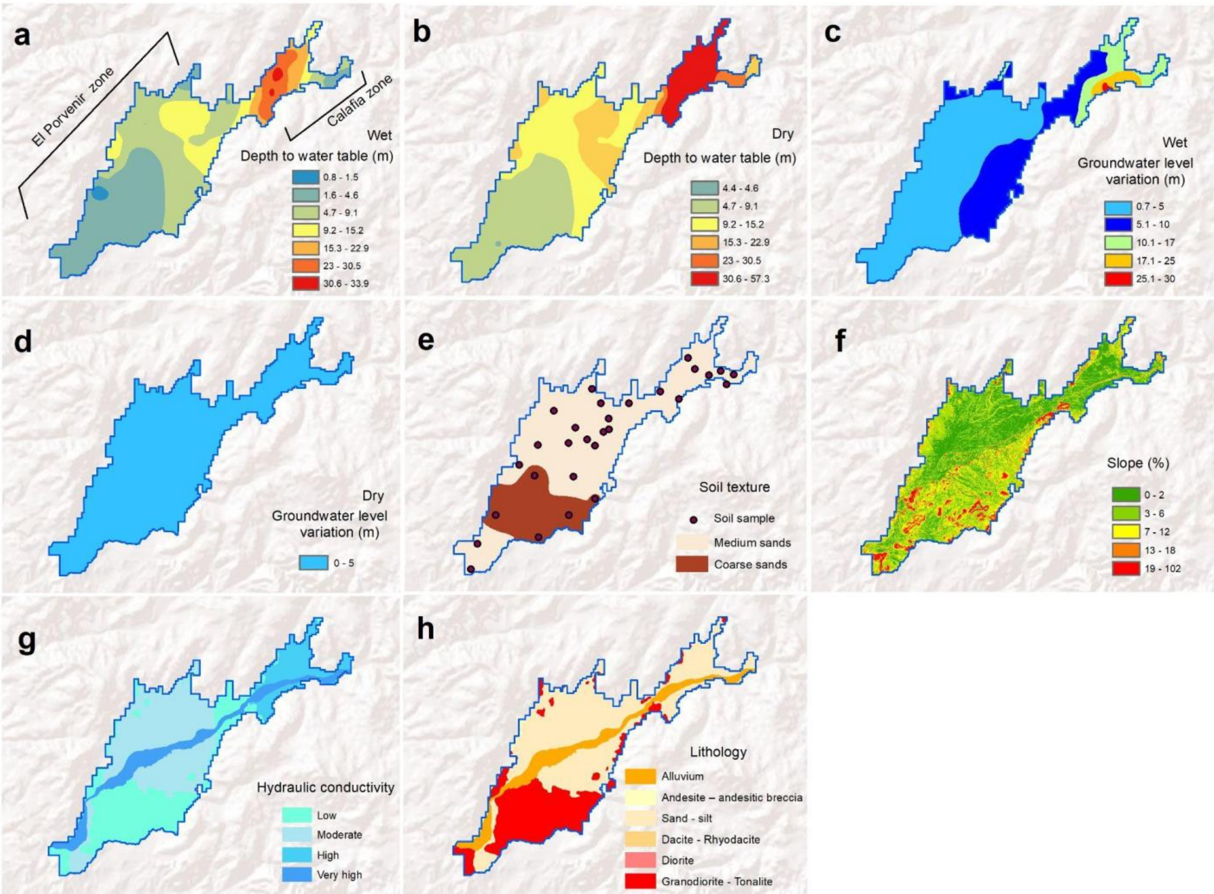

Figure 2. Characteristics of the study area. (**a**) = depth to water table in wet scenario, (**b**) = depth to water table in dry scenario, (**c**) = groundwater level variation in wet scenario, (**d**) = groundwater level variation in dry scenario, (**e**) = soil texture, (**f**) = slope, (**g**) = hydraulic conductivity, (**h**) = lithology.

In the study area (Figure 2g), low hydraulic conductivity is observed between the intersection of the zones (Calafia and El Porvenir) and to the south of the aquifer, representing 34.5%. Moderate conductivity extends over a large part of the center of El Porvenir with 40.5%, high hydraulic conductivity is located in the Calafia zone with 11.5% of the total study area, and finally, very high hydraulic conductivity is located in the course of the Guadalupe stream representing 13.5%.

According to [19], the lithology influences the infiltration and transport of potential contaminants from the surface to the saturated zone of the aquifer. In the study site, low permeable rocks cover 38% of the study area and are formed by granodiorite, andesite, diorite, and dacite, located towards the southwest and at the aquifer boundaries; the remaining area is covered by sands and silts constituting the permeable material [48], therefore, 62% of the surface is susceptible to the infiltration of contaminants (Figure 2h).

3.1. Vulnerability Ranking

In terms of area coverage, the depth to groundwater level (D) was classified into seven rankings: (1) <30.5 m; (2) 23–30.5 m; (3) 15.3–22.9 m; (5) 9.2–15.2 m; (7) 4.7–9.1 m;

(9) 1.6–4.6 m; (10) 0–1.5 m (Table 4), covering about 1%, 6%, 5%, 16%, 34%, 37%, and 1%, respectively, of the total study area in the wet scenario (Figure 3a).

Table 4. Numerical ranking factors (*Rj*) for each parameter used to calculate the DRASTIC vulnerability index (*DVI*) [23].

Depth to Water Table (D)		Recharge–Water Level Variation (R)		Aquifer Media (A)		Soil (S)	
Range (m)	**Rj**	**Range (m)**	**Rj**	**Type**	**Rj**	**Texture**	**Rj**
0–1.5	10	0–5	1	Granodiorite—Tonalite	3	Middle sands	9
1.6–4.6	9	5.1–10	3	Greenstone	3	Coarse sands	10
4.7–9.1	7	10.1–17	6	Dacite—Rhyodacite	3		
9.2–15.2	5	17.1–25	8	Andesite	4		
15.3–22.9	3	>25	9	Sand—Silt	8		
23–30.5	2			Alluvium	9		
>30.5	1						
Topography (T)		**Impact of the Vadose Zone (I)**		**Hydraulic Conductivity (C)**			
Range (%)	**Rj**	**Type**	**Rj**	**Category**	**Rj**		
0–2	10	Granodiorite—Tonalite	4	Low	4		
2–6	9	Diorite		Moderate	6		
6–12	5	Dacite—Rhyodacite	4	High	8		
12–18	3	Andesite	4	Very High	10		
> 18	1	Sand—Silt	4				
		Alluvium	6				
			8				

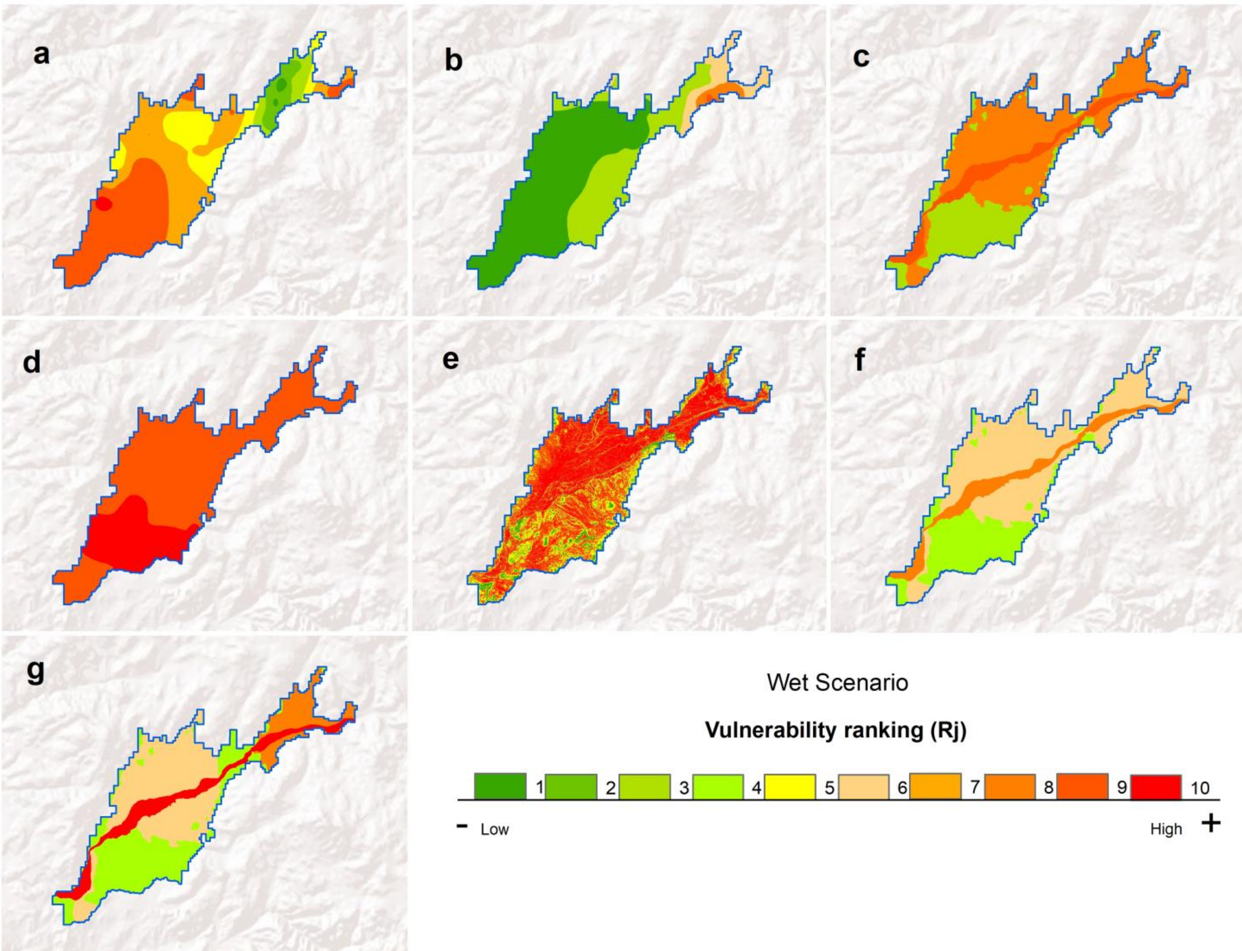

Figure 3. DRASTIC parameters during the wet scenario. (**a**) = depth to water table, (**b**) = recharge–water level variation, (**c**) = aquifer media, (**d**) = soil, (**e**) = topography, (**f**) = impact of the vadose zone, (**g**) = hydraulic conductivity.

On the other hand, in the dry scenario, D was classified into six rankings: (1) <30.5 m; (2) 23–30.5 m; (3) 15.3–22.9 m; (5) 9.2–15.2 m; (7) 4.7–9.1 m; (9) and 1.6–4.6 m (Table 4), covering about 12%, 3%, 18%, 31%, 35%, and 1%, respectively, of the total study area in the dry scenario (Figure 4a).

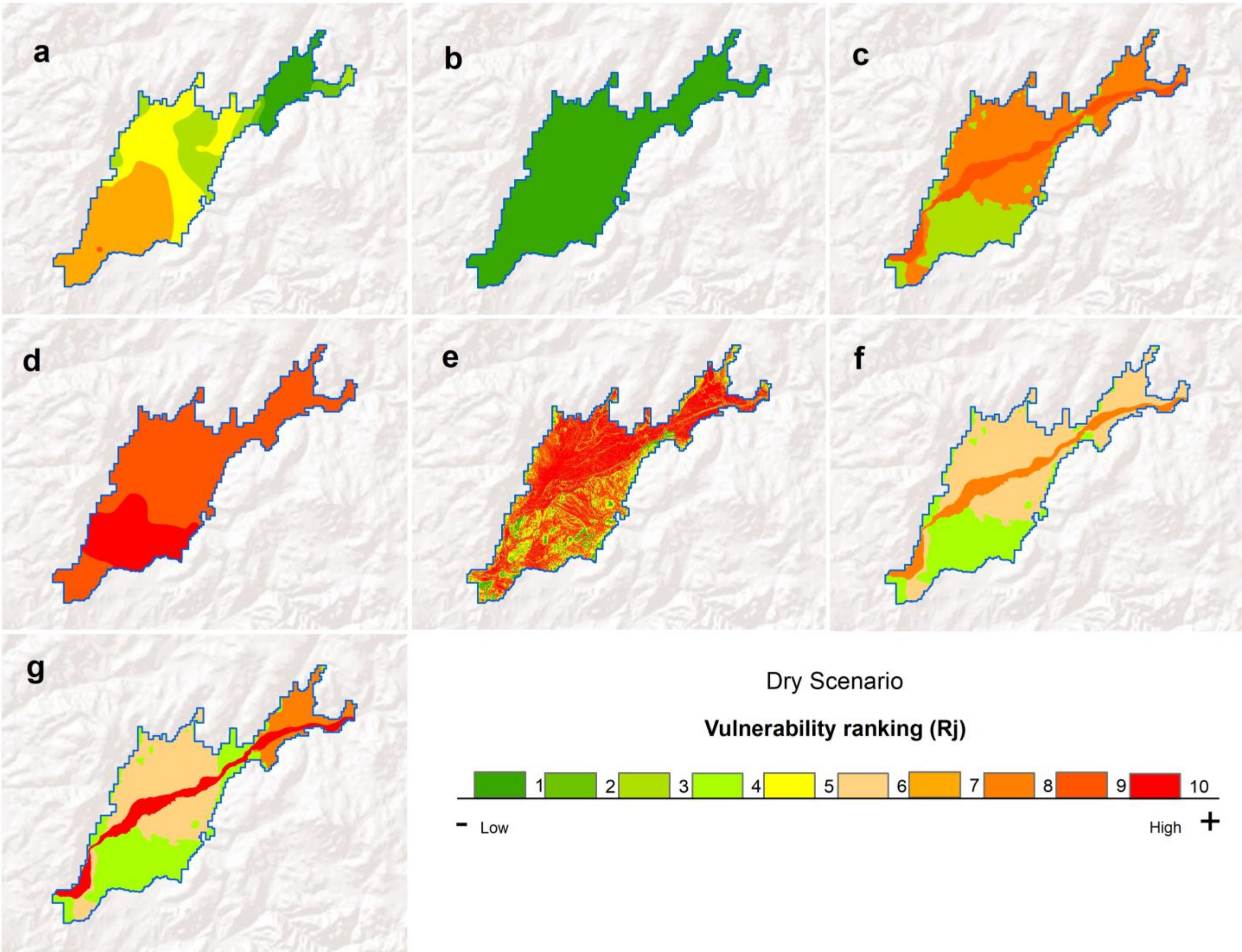

Figure 4. DRASTIC parameters during the dry scenario. (**a**) = depth to water table, (**b**) = recharge–water level variation, (**c**) = aquifer media, (**d**) = soil, (**e**) = topography, (**f**) = impact of the vadose zone, (**g**) = hydraulic conductivity.

The level of variation (R) was classified into five rankings: (1) 0–5 m; (3) 5.1–10 m; (6) 10.1–17 m; (8) 17.1–25 m; (9) 4.7–9.1 m; (9) >25 m (Table 4), covering about 61%, 27%, 8%, 3%, and 1%, respectively, of the total study area in the wet scenario (Figure 3a) and 100% for ranking (1) in the dry scenario (Figure 4a).

The following parameters in both scenarios have the same categories, as they are constant over time. The aquifer environment (A) was classified into four rankings: (3) Granodiorite—Tonalite, Greenstone, and Dacite—Rhyodacite; (4) Andesite; (8) Sand—Silt; (9) Alluvium (Table 4), covering about 30%, 1%, 56%, and 13%, respectively, of the total study area (Figures 3c and 4c).

Soil texture (S) was classified into only two rankings: (9) Middle sands and (10) Coarse sands (Table 4), covering about 76% and 24%, respectively, of the total study area (Figures 3d and 4d).

Topography (T) was classified into five rankings by percentage: (10) 0–2%; (9) 2–6%; (5) 6–12%; (3) 12–18%; (1) >18% (Table 4), covering about 33%, 38%, 8%, 10%, and 11%, respectively, of the total study area (Figure 3a).

The impact in the vadose zone (I) was classified into three rankings: (4) Granodiorite—Tonalite, Diorite, and Dacite—Rhyodacite; (6) Andesite; (8) Sand—Silt and Alluvium (Table 4) covering about 31%, 56%, and 13%, respectively, of the total study area (Figures 3f and 4f).

Hydraulic conductivity (C) was classified into four rankings: (4) low; (6) moderate; (8) high; and (10) very high (Table 4), covering about 34%, 41%, 12%, and 13%, respectively, of the total study area (Figures 3g and 4g).

The DRASTIC method was applied to create seven maps for wet and dry scenarios (Figures 3 and 4) with rankings of each parameter of Table 4.

3.2. Vulnerability to Pollution of the Guadalupe Aquifer, Application of the DRASTIC Method

Figures 5 and 6 show the vulnerability level maps of the GA aquifer using the DRASTIC method. The vulnerability level scores in the wet scenario, obtained from the model, showed a unimodal distribution from 82 to a maximum of 202 and those in the dry scenario from a minimum of 69 to 176. The ranges in these scenarios go from 69–105 (low), 106–146 (moderate), 147–187 (high), and 188–202 (very high). The area corresponding to each vulnerability class is shown in Table 5.

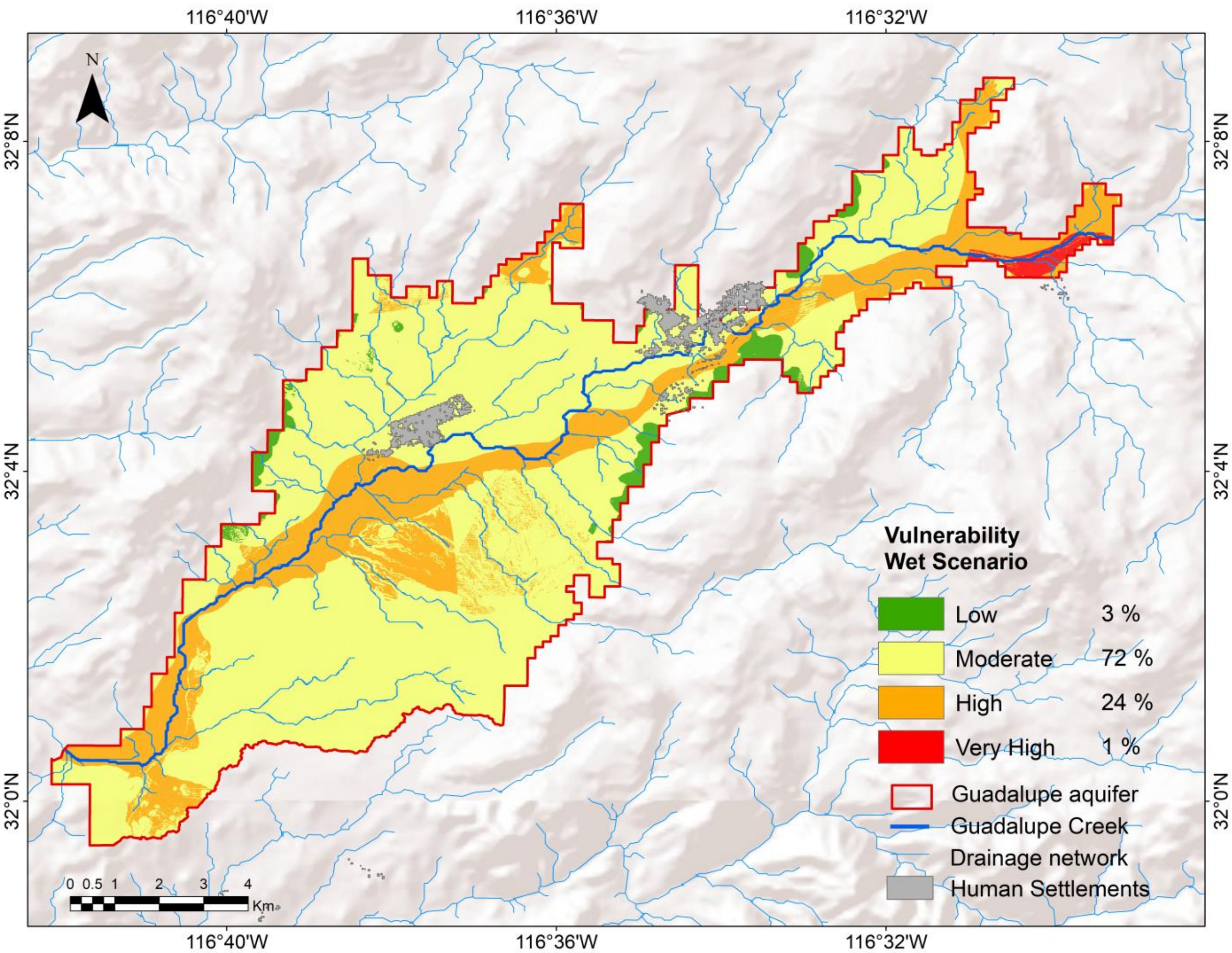

Figure 5. Vulnerability to pollution level in the wet scenario, application of the DRASTIC method.

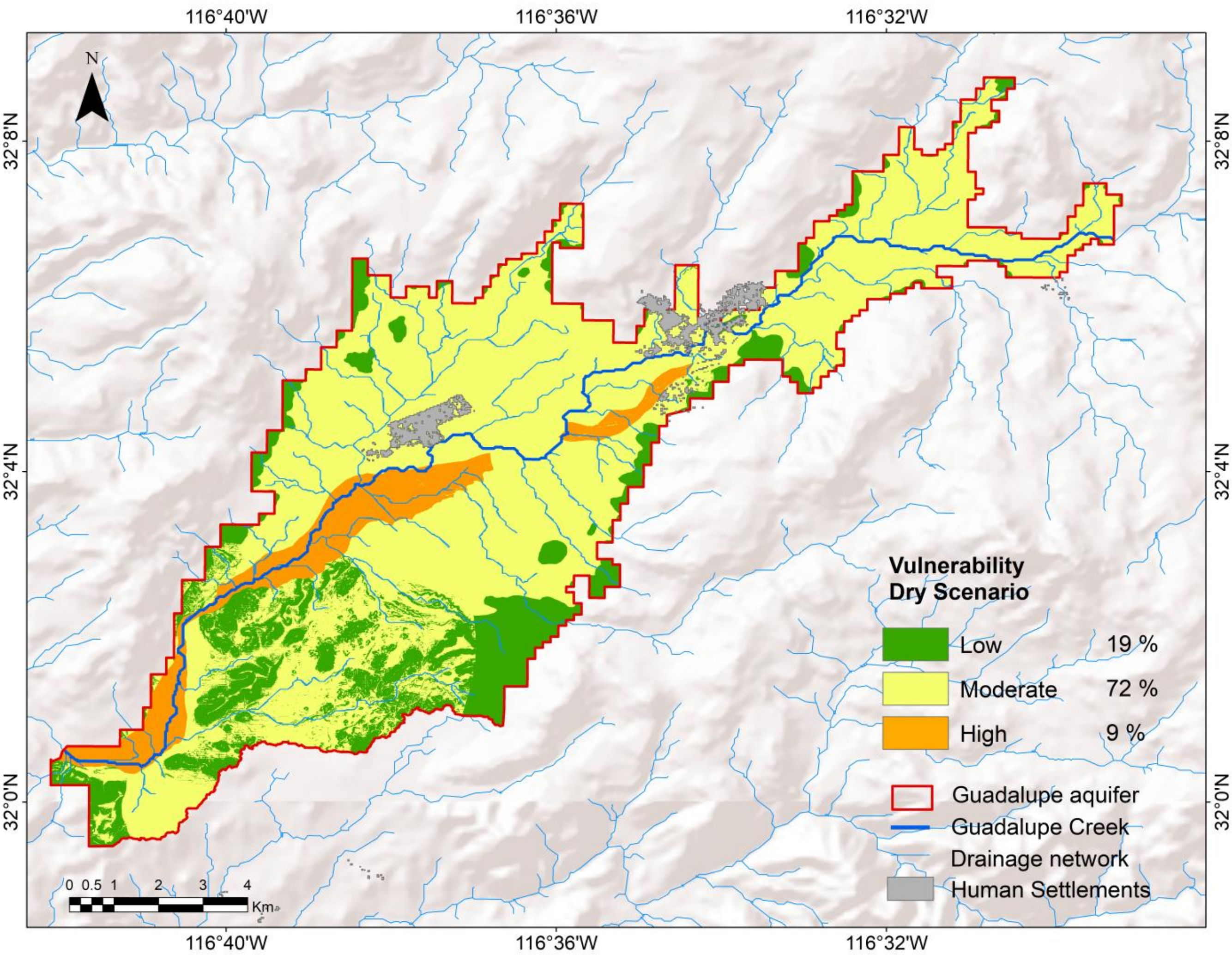

Figure 6. Vulnerability to pollution level in the dry scenario, application of the DRASTIC method.

Table 5. Area under vulnerability to groundwater pollution in the Guadalupe Aquifer. DVI results in the wet and dry scenarios.

Class Number	Vulnerability	DRASTIC Index Value	Dry Scenario Area (%)	Wet Scenario Area (%)
1	Low	65–105	19	3
2	Moderate	106–146	72	72
3	High	147–187	9	24
4	Very high	188–230	0	1

3.2.1. Wet Scenario

In the wet scenario (Figure 5), the predominant vulnerability zones are classified as moderate according to the resulting map, representing 72% of the GA area (yellow). The depth and water level variation were important parameters for the application of the method, as they are dynamic over time. The results show a range of very high and high vulnerability (red and orange) in the northeastern Calafia area due to the greater water level depth. Likewise, vulnerability is high along the stream bed, considering that this is where the significant accumulation of water and higher hydraulic conductivities are found compared to the rest of the area. It should also be considered that important wells for water extraction for agricultural irrigation are located near these areas' streams. The green areas represent a low vulnerability; mainly due to the type of semi-permeable to impermeable geological material (granodiorite, tonalite, or diorite), they are located at the extremes of the study area.

3.2.2. Dry Scenario

According to the resulting map (Figure 6), only three vulnerability classes are shown, explained by the fact that the unsaturated zone is quite thick. The low vulnerability category (19%) is mainly distributed in the south of the aquifer (green color) and in the extreme zones of the GA, where the geological material of granodiorite and diorite is found and is absent in the central area of the "El Porvenir and Calafia" zone. However, more than half of the study area (72%) is classified as moderately vulnerable (yellow color); this category is distributed along the aquifer but predominates most of the center of "El Porvenir", except some areas of the stream. In "Calafia" the moderate category covers the whole center of the zone. The highest indices are calculated for some parts of the center following the course of the stream to the south, which are therefore considered to be of high vulnerability (9%, orange color) due to very permeable areas of coarse sands, high hydraulic conductivity, and smaller level depths (maximum of 5.8 m for the El Porvenir area) concerning the other areas.

3.3. Nitrate Concentration (NO_3^-)

In a pollution vulnerability model, analyzing its results with a parameter representing a potential pollutant is essential. In the present study, groundwater nitrate concentration data from different sites for the years 2001, 2020, and 2021 were used to validate the vulnerability of the aquifer based on the application of the DRASTIC method. Table 6 shows the descriptive statistics of the nitrate concentration results.

Table 6. Nitrate concentration (NO_3^-) in the Guadalupe Aquifer.

Year	Number of Samples	Concentration NO_3^- (mg L^{-1})			
		Min	**Max**	**Mean**	**Standard Deviation**
2001 [44]	27	0.44	115.13	26.56	26.29
2020	33	0.25	131.19	19.90	30.82
2021	28	0.08	128.95	30.74	34.76

At some points of the groundwater samples from wells, the spatial distribution of nitrate concentrations exceeds the values recommended by the Mexican Official Standard for water for human consumption NOM-127-SSA1-2021. Concentrations reach maximum values of up to 131.19 mg L^{-1}. NO_3^-).

A spatial distribution analysis was carried out, where nitrate concentrations were classified in categories using the traffic light technique. The criteria used for the creation of categories were empirically based on the nitrate concentration thresholds established by the permissible limits for drinking water by the NOM-127-SSA1-2021, half of this limit, and the minimum detected in the samples analyzed. Table 7 shows the different categories: good—green from 0.44 to 24.31 mg L^{-1} (indicates a state of equilibrium and compliance with the permissible limits established by the standard), regular—yellow from 24.32 to 48.62 mg L^{-1} (complies with the maximum permissible limits), bad—orange from 48.63 to 97.24 mg L^{-1} (exceeds the quality indicators for human use and consumption) and very bad—red from 97.25 to 131.19 mg L^{-1} (exceeds the permissible limits, in a critical state).

The observed high nitrate concentrations in specific sampled sites are likely attributed to the infiltration of water combined with fertilizers from the agricultural areas and their expansion in the Guadalupe Valley and probably also urban wastewaters near the settlements. Further assessment wit nitrogen stable isotopes would be required to further assess the sources of nitrate.

Areas of high and very high vulnerability indicate groundwater contamination and could be further worsened by agrochemicals as it is an important agricultural area. Nitrates naturally occur at very low concentrations in groundwater, but an increasing trend indicates pollution.

Table 7. Nitrate concentration categories according to NOM-127-SSA1-2021 [35].

	Color	Categories	Min	Max
●	Green	Good	0.44	24.31
●	Yellow	Fair	24.32	48.62
●	Orange	Bad	48.63	97.24
●	Red	Very bad	97.25	131.19

To compare the groundwater system's pollution state with the vulnerability zones, we used the concentration of nitrate (NO_3^-). After overlaying the concentrations with the vulnerability map for 2001 (Figure 7), only two sites with a "very bad" concentration (red) are present, i.e., exceeding the permissible limits for water for human use and consumption, according to NOM-127-SSA1-2021. These sites are located in the center of the El Porvenir area, where the most predominant activity is agriculture and where, according to the aquifer contamination vulnerability analysis, it is of moderate vulnerability, bordering the high vulnerability zone. For the same year, there are ten sites with "fair" nitrate concentrations (yellow); six in the Calafia area and four in El Porvenir, where three coincide with high vulnerability zones. Fifteen of them are in the "good" (green) category, and eleven are located in the Calafia zone, in moderate and high vulnerability areas.

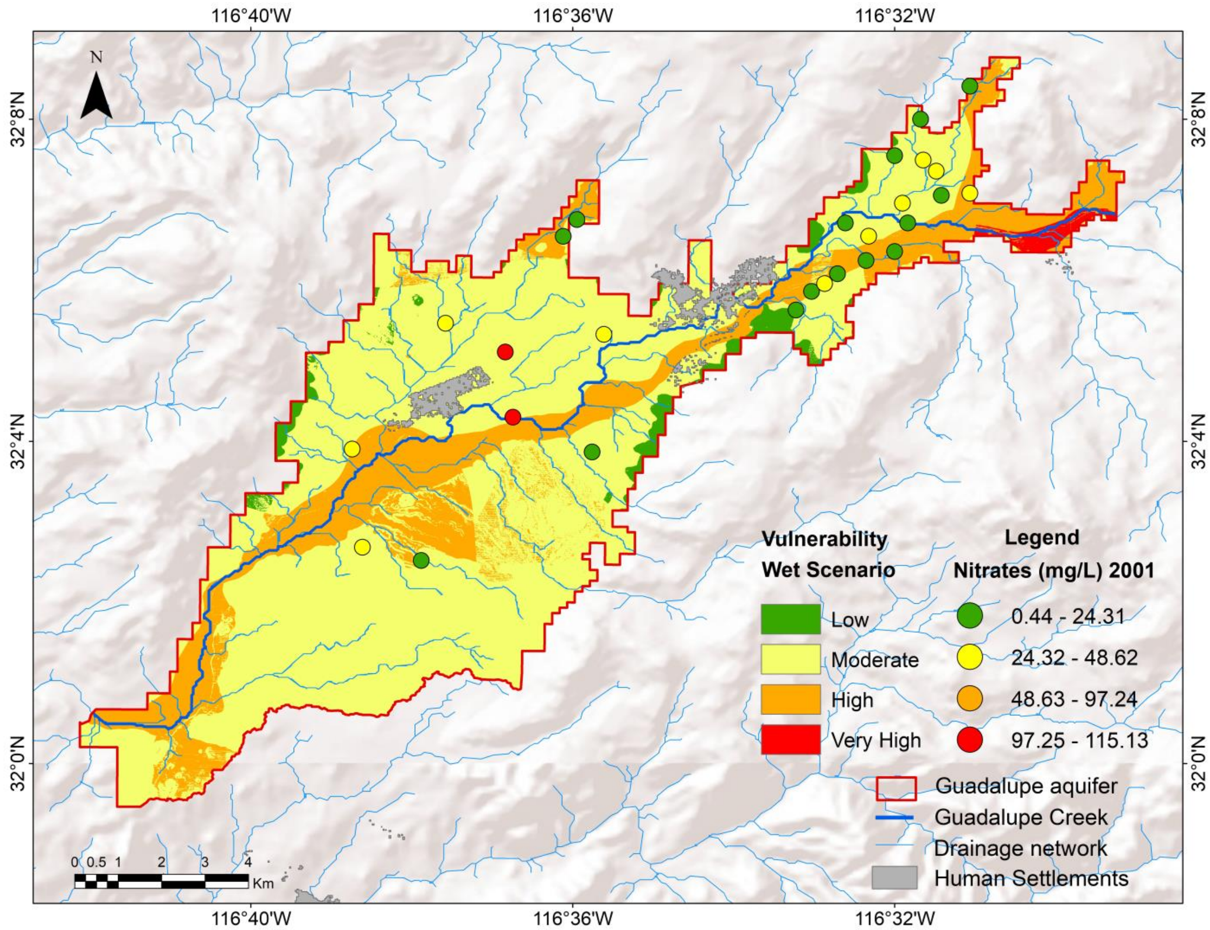

Figure 7. Nitrate concentration 2001 with areas of vulnerability levels to aquifer pollution.

The distribution and concentration of nitrate in 2020 (Figure 8) show in the center and southwest of the aquifer, the concentrations of two sites in the "very bad" category (red), which indicate very high nitrate concentration levels; and one of them is located in the southwest zone of the Guadalupe stream with a high vulnerability type, and the other is located between the urban zone and the stream, in the center of the El Porvenir zone, falling in a moderate vulnerability type. This year there are no nitrate concentrations in the "bad" category (orange) and seven sites in the regular category (yellow); of these seven, five are in areas of high vulnerability to pollution, following the course of the stream, and two fall into moderate vulnerability. The remaining twenty-four samples correspond to the good category; three of them fall in zones of very high vulnerability to the northeast of the Calafia zone, twelve samples fall on or near high vulnerability zones, and the rest randomly fall in moderate vulnerability zones.

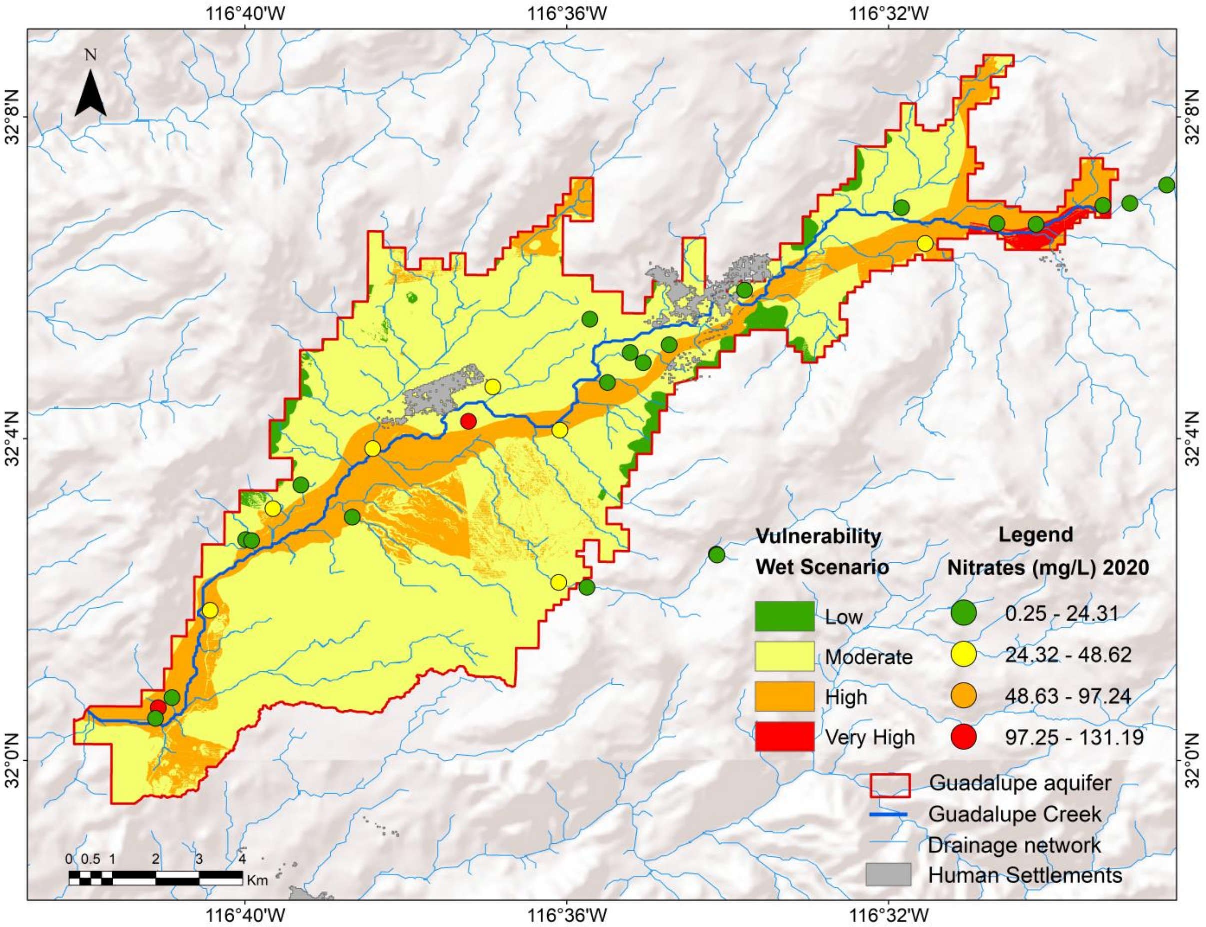

Figure 8. Nitrate concentration 2020 with areas of vulnerability levels to aquifer pollution.

For 2021 (Figure 9), the four categories assigned to nitrate concentration were detected. Three samples are in the "very bad" category (red); the first is located in the center, between the stream and the urban area, in an area of moderate vulnerability, and the other two are located southwest of the stream in an area of high vulnerability, coinciding with some of them changing negatively in category over time, starting in the area of El Porvenir, until the end of the stream channel shown in the map, exceeding the permissible limits and coinciding with a high vulnerability to pollution of the aquifer. Three samples in the "bad" concentration category (orange) are in or very close to the stream's course, with a moderate vulnerability type and one in high vulnerability. On the other hand, seven samples were found in the "regular" category (yellow); five fall into moderate vulnerability zones and two are in high vulnerability. Finally, the remaining 15 nitrate concentration samples that are in the "good" (green) category, which is equivalent to an acceptable nitrate concentration for the site, are distributed along the course of the stream, located between the moderate and high vulnerability zones, and two samples at the limits of very high vulnerability.

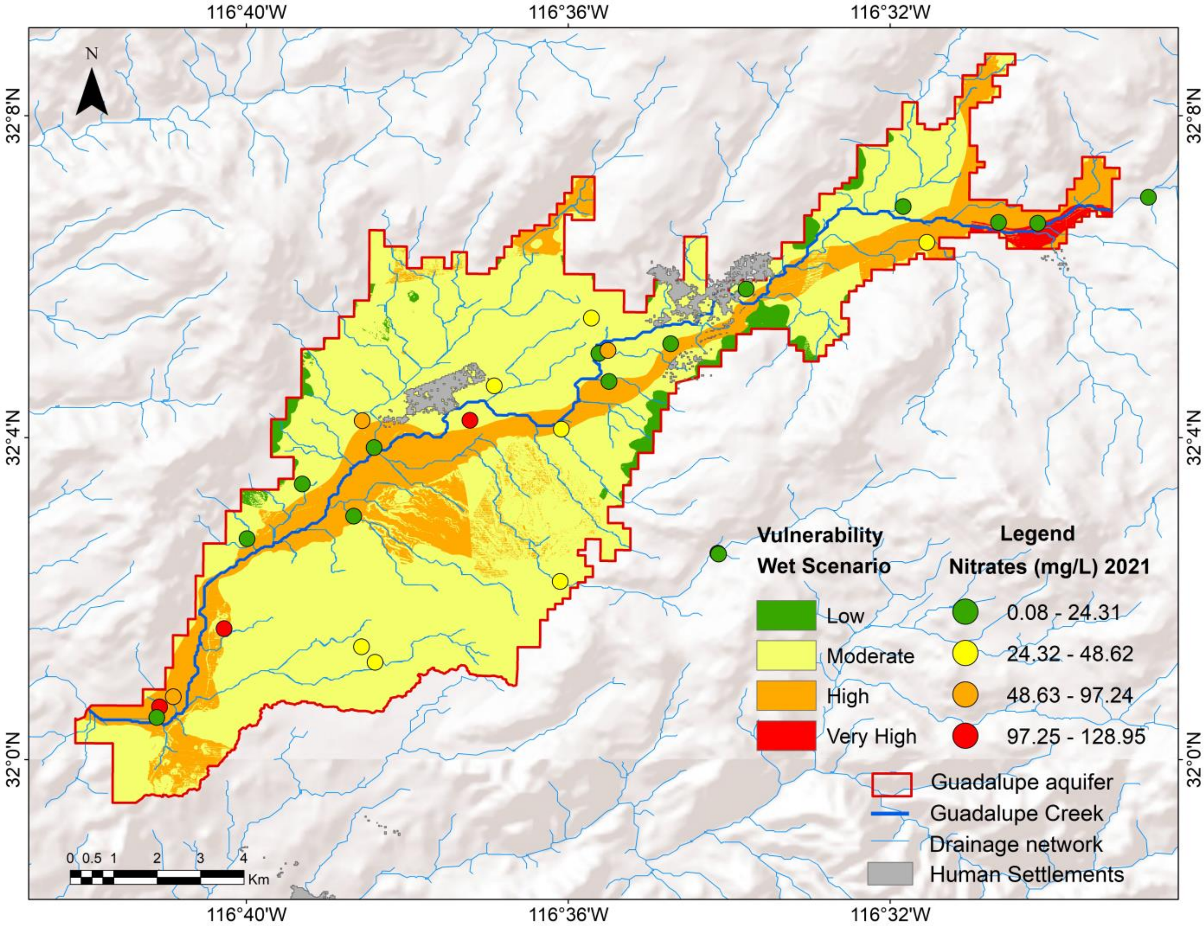

Figure 9. Nitrate concentration 2021 with areas of vulnerability levels to aquifer pollution.

The resulting groundwater vulnerability zones were verified using the AUC (area under the curve) [59] based on nitrate concentration data for the year 2021. Figure 10 shows the estimated AUC validation curve for the DRASTIC vulnerability map. The AUC values were 0.597 on the vulnerability category scale. The highest values of the AUC curve demonstrated that the method applied to predict the moderate category vulnerability of aquifers has an acceptable fit to the results. However, this is not the case for high-vulnerability areas. According to information published by [11], water flow direction in the GA has a general direction from NE to NW, with a focused N-S direction in the Porvenir zone regions caused by a steep decrease in water table levels due to intense pumping. In this specific site, categories of moderate and high vulnerability to contamination were observed (on the course of the Guadalupe stream), as well as high levels of nitrate concentration. Furthermore, a land use and vegetation map of the GV (Figure 11) shows that there is now evident correlation between land use and nitrate concentrations for the same year, as well as the regional distribution of nitrate concentrations for the same year. A much higher resolution of water samples is required to fully assess factors influencing the distribution of nitrate concentrations.

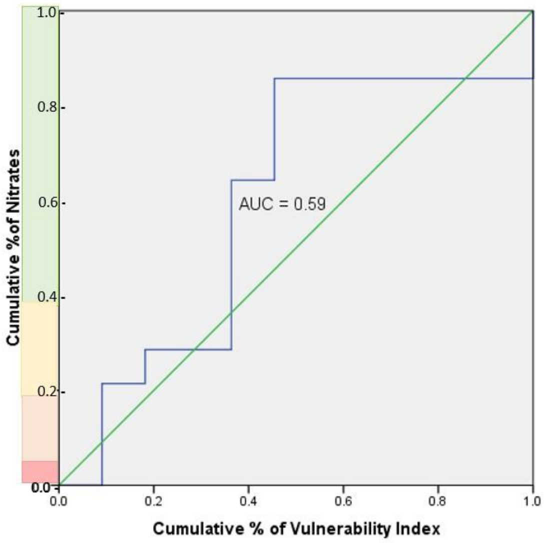

Figure 10. DRASTIC vulnerability index using nitrate concentrations for 2021. The blue line refers to the ROC (Receiver Operating Characteristics) curve and the green line is a reference to obtain the AUC (area under the curve).

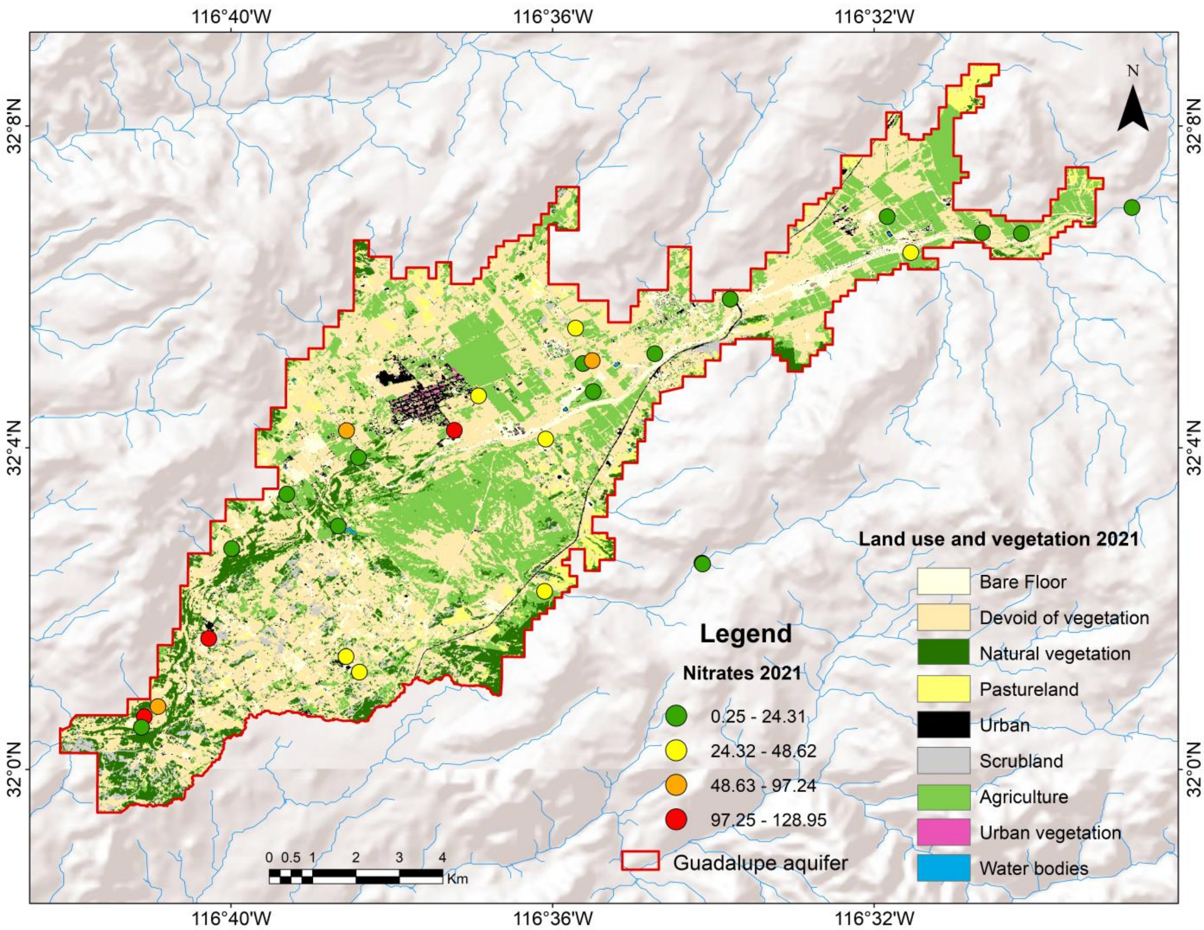

Figure 11. Land use and vegetation in the Guadalupe Valley with nitrate concentrations in 2021. Prepared by the authors with Google Earth Engine, based on [60].

4. Limitations and Recommendations

Despite its advantages as an integrated approach to assess groundwater vulnerability across multiple layers, the DRASTIC method has challenges. A significant limitation emerges when essential data for aquifer assessment, such as precise aquifer lithology and vertical hydraulic conductivity, are unavailable. Information is necessary to ensure the accuracy of the DRASTIC assessment. Another consideration is the method's reliance on assigned weights and numerical values for each indicator, introducing subjectivity into the results. The method's applicability is context-dependent, demanding a nuanced understanding of site-specific characteristics, particularly the primary activities in the area that could influence the aquifer. In our specific case, a key constraint lies in the availability of up-to-date hydrogeological data. Emphasizing these limitations underscores the need for continuous efforts to enhance data quality and availability in the GA. Furthermore, the transport of contaminants, like nitrate, can be influenced by microbial activity, geochemical reactions, and/or subsurface heterogeneity, and their possible sources such as fertilizers, wastewater, or manure need to be assessed in more detail. All these biases and gaps in information need to be considered in order to increase the reliability on vulnerability methods used for management purposes. Future research should focus on monitoring and mitigating sources of nitrate pollution and exploring additional parameters to improve the accuracy of vulnerability assessments. In potentially vulnerable locations, preventive and management measures must be taken in the aquifer through restrictions on groundwater abstraction and moderation of agrochemical use in predominantly agricultural regions. It is also essential to closely monitor groundwater quality (on a higher resolution) and variation to generate detailed information for further studies in the AG.

5. Conclusions

The resulting DRASTIC map of vulnerability to groundwater pollution of the study area for two scenarios (wet and dry) revealed that there are different zones of vulnerability. depending mainly on the depth of groundwater level and the variation of groundwater level from one season to another, also obtaining a significant variation in the values of the index when the zones have different geological, sedimentological, slope, and conductivity characteristics. Specifically, the pollution vulnerability map in the wet scenario revealed that alluvial areas with shallow depths (where groundwater is closer to the land surface) have the highest vulnerability indices. In contrast, areas with steeper slopes, less porosity, or shallower permeable material and deeper depths have the lowest vulnerability indices.

With the application of the DRASTIC method, "very high" vulnerabilities were found in the northwest area of Calafia with dimensionless values from 188 to 202. According to the method, the maximum possible value would be 230. Although the maximum value of 230 was not reached in any scenario, a worse scenario (more areas of "very high" vulnerability) could still occur if groundwater levels were to increase, resulting in a lower thickness in the vadose zone. The results indicate varying degrees of vulnerability in the Guadalupe Valley aquifer. High vulnerability zones were identified in areas with shallow groundwater depth, permeable soils, and high nitrate concentrations. These zones coincide with regions of intense agricultural activity, suggesting a direct relationship between anthropogenic practices and aquifer contamination. In contrast, low-vulnerability areas were characterized by deep groundwater levels, impermeable soils, and minimal nitrate concentrations. According to the method and the results of the vulnerability map, the determining indicators to indicate possible areas prone to contamination are the depth level and the geology in the vadose zone.

In the Calafia zone, to the northeast of the aquifer, zones of "very high" vulnerability to pollution were found; however, high concentrations of nitrates were not found because it is one of the leading recharge zones with greater level variation, which allows the available water to serve for the diffusion and dilution of contaminants by a greater flow velocity, as it has high hydraulic conductivity and short residence times. The zones with very high vulnerability have a shallower depth (0.8 to 4.6 m), shallow slopes (0 to 6%), and alluvial material to the northeast of the aquifer.

The vulnerability maps of the GA provide information on the areas susceptible to pollution, considering the scenarios (wet and dry), which coincide mostly in the areas of high and very high vulnerability, with a tendency to increase in areas of vulnerability. As for water quality, which was compared taking into account the concentration of nitrate, its behavior is increasing over time, significantly increasing in areas of high and moderate vulnerability, which indicates the presence of pollutants of anthropogenic origin. The site with the highest nitrate concentrations for the years 2020 and 2021 (131.19 and 128.95 mg L^{-1}, respectively) is located in the center of the aquifer, very close to the stream, where there are maximum water table depths of 9 m and minimal level variation, in the porous medium there is alluvium, medium to coarse sands and silt, and topographic slopes of 0 to 6% predominate. These characteristics indicate a site prone to high infiltration of pollutants and long residence times.

Integrating the DRASTIC method with nitrate analysis provided a local understanding of the aquifer's vulnerability to pollution. The results can be relevant inputs for land-use planning, groundwater management strategies, and the implementation of preventive measures to safeguard the water resources of the Guadalupe Valley.

Author Contributions: Conceptualization, G.D.-G., F.J.D.-T.-G. and L.W.D.; methodology, G.D.-G.; investigation, G.D.-G.; resources, L.W.D.; data curation, G.D.-G.; writing—original draft preparation, G.D.-G.; writing—review and editing, L.W.D., F.J.D.-T.-G., M.V.-C. and G.S.; funding acquisition, L.W.D. All authors have read and agreed to the published version of the manuscript.

Funding: This research was funded by the Consejo Nacional de Humanidades, Ciencia y Tecnología (CONAHCYT) Project Number: A1-S 22656, IRADES.

Data Availability Statement: The data presented in this study are available on request from the corresponding author.

Acknowledgments: We thank the National Council for Humanities, Science and Technology (CONA HCYT) for the support provided to this research, through the project grant A1-S 22656, IRADES and a scholarship to G.D.G for her PhD studies. We thank PRODEP and CONAHCYT for postdoctoral grants for F.T.G at UABC. Also, J. Lafarga for sharing the groundwater depth information collected by COTAS Guadalupe.

Conflicts of Interest: The authors declare no conflict of interest.

References

1. Paris, M. *La Seguridad Hídrica y Los Objetivos de Desarrollo Sostenible Manual de Capacitación Para Tomadores de Decisión. La Seguridad*; UNESCO, United Nations Educational, Scientific and Cultural Organisation: Montevideo, Uruguay, 2020; Volume 53.
2. FAO. *The State of the World's Land and Water Resources for Food and Agriculture (SOLAW)*; FAO: Rome, Italy, 2011; ISBN 9781849713269.
3. Havryliuk, R.; Savchenko, S. Water Resources Assessment. In *Clean Water and Sanitation*; Springer International Publishing: Cham, Switzerland, 2022; pp. 871–883. [CrossRef]
4. Gale, I.; Dillon, P. *Strategies for Managed Aquifer Recharge (MAR) in Semi-Arid Areas*; Gale, I., Ed.; United Nations Educational, Scientific, and Cultural Organization (UNESCO): Paris, France, 2005; pp. 1–33.
5. Hernández, R.; Martínez, L.; Peñuela, L.; Rivera, S. Gestión Del Agua Subterránea En Los Acuíferos de La Cuenca Del Río Ayuquila-Armería En Jalisco y Colima, México. *Región Y Soc.* **2019**, *31*, 26. [CrossRef] [PubMed]
6. Foster, S.; Hirata, R. Determinación Del Riesgo de Contaminación de Aguas Subterráneas: GOD. *Cent. Panam. Ing. Sanit. y Ciencias Ambient./Organ. Mund. Salud* **1991**, *2*, 80.
7. Su, C.; Li, Z.; Wang, W.; Cheng, Z.; Zheng, Z.; Chen, Z. Key Factors Dominating the Groundwater Chemical Composition in a Grain Production Base: A Case Study of Muling–Xingkai Plain, Northeast China. *Water* **2022**, *14*, 2222. [CrossRef]
8. Merem, E.; Yerramilli, S.; Twumasi, Y.; Wesley, J.; Robinson, B.; Richardson, C. The Applications of GIS in the Analysis of the Impacts of Human Activities on South Texas Watersheds. *Int. J. Environ. Res. Public Health* **2011**, *8*, 2418–2446. [CrossRef]
9. Bortolini, L.; Maucieri, C.; Borin, M. A Tool for the Evaluation of Irrigation Water Quality in the Arid and Semi-Arid Regions. *Agronomy* **2018**, *8*, 23. [CrossRef]
10. Huang, T.; Pang, Z.; Edmunds, W.M. Soil Profile Evolution Following Land-Use Change: Implications for Groundwater Quantity and Quality. *Hydrol. Process.* **2012**, *27*, 15. [CrossRef]
11. Daesslé, L.W.; Andrade-Tafoya, P.D.; Lafarga-Moreno, J.; Mahlknecht, J.; van Geldern, R.; Beramendi-Orosco, L.E.; Barth, J.A.C. Groundwater Recharge Sites and Pollution Sources in the Wine-Producing Guadalupe Valley (Mexico): Restrictions and Mixing Prior to Transfer of Reclaimed Water from the US-México Border. *Sci. Total Environ.* **2020**, *713*, 136715. [CrossRef]

12. Rakotondrabe, F.; Ngoupayou, J.; Mfonka, Z.; Rasolomanana, E.H.; Nyangono Abolo, A.J.; Asone, B.L.; Ako Ako, A.; Rakotondrabe, M.H. Assessment of Surface Water Quality of Bétaré-Oya Gold Mining Area (East-Cameroon). *J. Water Resour. Prot.* **2017**, *9*, 960–984. [CrossRef]
13. Gogu, R.; Dassargues, A. Current Trends and Future Challenges in Groundwater Vulnerability Assessment Using Overlay and Index Methods. *Environ. Geol.* **2000**, *39*, 549–559. [CrossRef]
14. Foster, S.; Hirata, R.; Gomes, D.; D'Elia, M.; Paris, M. Groundwater Quality Protection: A Guide for Water Utilities, Municipal Authorities, and Environment Agencies. World Bank: Washington, DC, USA, 2003; ISBN 84-8476-146-0.
15. Orellana, J.; Perles, M.; Causapé, J. A Methodology for Assessing Groundwater Pollution Hazard by Nitrates from Agricultural Sources: Application to the Gallocanta Groundwater Basin (Spain). *Sustainability* **2021**, *13*, 6321. [CrossRef]
16. Nadiri, A.A.; Norouzi, H.; Khatibi, R.; Gharekhani, M. Groundwater DRASTIC Vulnerability Mapping by Unsupervised and Supervised Techniques Using a Modelling Strategy in Two Levels. *J. Hydrol.* **2019**, *574*, 744–759. [CrossRef]
17. Elçi, A. Calibration of Groundwater Vulnerability Mapping Using the Generalized Reduced Gradient Method. *J. Contam. Hydrol.* **2017**, *207*, 39–49. [CrossRef]
18. Bhuvaneswaran, C.; Ganesh, A. Spatial Assessment of Groundwater Vulnerability Using DRASTIC Model with GIS in Uppar Odai Sub-Watershed, Nandiyar, Cauvery Basin, Tamil Nadu. *Groundw. Sustain. Dev.* **2019**, *9*, 14. [CrossRef]
19. Aller, L.; Bennett, T.; Lehr, J.H.; Petty, R.J.; Hackett, G. *DRASTIC: A Standardized Method for Evaluating Ground Water Pollution Potential Using Hydrogeologic Settings*; Environmental Research Laboratory Office of Reseach and Development U.S.: Dublin, OH, USA, 1987.
20. Bai, L.; Wang, Y.; Meng, F. Application of DRASTIC and Extension Theory in the Groundwater Vulnerability Evaluation. *Water Environ. J.* **2012**, *26*, 381–391. [CrossRef]
21. Meng, L.; Zhang, Q.; Liu, P.; He, H.; Xu, W. Influence of Agricultural Irrigation Activity on the Potential Risk of Groundwater Pollution: A Study with Drastic Method in a Semi-Arid Agricultural Region of China. *Sustainability* **2020**, *12*, 1954. [CrossRef]
22. Abdeslam, I.; Fehdi, C.; Djabri, L. Application of Drastic Method for Determining the Vulnerability of an Alluvial Aquifer: Morsott—El Aouinet North East of Algeria: Using Arcgis Environment. *Energy Procedia* **2017**, *119*, 308–317. [CrossRef]
23. Neshat, A.; Pradhan, B.; Dadras, M. Groundwater Vulnerability Assessment Using an Improved DRASTIC Method in GIS. *Resour. Conserv. Recycl.* **2014**, *86*, 74–86. [CrossRef]
24. Jia, Z.; Bian, J.; Wang, Y.; Wan, H.; Sun, X.; Li, Q. Assessment and Validation of Groundwater Vulnerability to Nitrate in Porous Aquifers Based on a DRASTIC Method Modified by Projection Pursuit Dynamic Clustering Model. *J. Contam. Hydrol.* **2019**, *226*, 103522. [CrossRef]
25. Hernández, A.; Reyna, A.; Sánchez, E.; Cabral, E.; Carrera, J.; Martínez, P.; Macías, S.; Falorni, G.; Colombo, D. The DRASTIC-Sg Model: An Extension to the DRASTIC Approach for Mapping Groundwater Vulnerability in Aquifers Subject to Differential Land Subsidence, with Application to Mexico City. *Hydrogeol. J.* **2014**, *22*, 1469–1485. [CrossRef]
26. Franco Plata, R. Adecuación del Método de Evaluación de Vulnerabilidad de Acuíferos (DRASTIC), Mediante el Uso del Trazado de Partículas en el Acuífero del Curso Alto Del Río Lerma, Estado de México. Master's Thesis, Universidad Autónoma del Estado de México, Toluca, Mexico, 2002.
27. Hasan, M.; Islam, M.A.; Aziz Hasan, M.; Alam, M.J.; Peas, M.H. Groundwater Vulnerability Assessment in Savar Upazila of Dhaka District, Bangladesh—A GIS-Based DRASTIC Modeling. *Groundw. Sustain. Dev.* **2019**, *9*, 100220. [CrossRef]
28. Pacheco, F.A.L.; Martins, L.M.O.; Quininha, M.; Oliveira, A.S.; Sanches Fernandes, L.F. Modification to the DRASTIC Framework to Assess Groundwater Contaminant Risk in Rural Mountainous Catchments. *J. Hydrol.* **2018**, *566*, 175–191. [CrossRef]
29. Ceballos, R.P.; Ávila, J.P. Vulnerabilidad Del Agua Subterránea a La Contaminación de Nitratos En El Estado de Yucatán. *Ingeniería* **2004**, *8*, 33–42.
30. Liang, J.; Li, Z.; Yang, Q.; Lei, X.; Kang, A.; Li, S. Specific Vulnerability Assessment of Nitrate in Shallow Groundwater with an Improved DRSTIC-LE Model. *Ecotoxicol. Environ. Saf.* **2019**, *174*, 649–657. [CrossRef]
31. Mfonka, Z.; Ndam Ngoupayou, J.R.; Kpoumie, A.; Ndjigui, P.D.; Zammouri, M.; Ngouh, A.N.; Mouncherou, O.F.; Mfochivé, O.F.; Rakotondrabe, F. Hydrodynamic and Groundwater Vulnerability Assessment of the Shallow Aquifer of the Foumban Locality (Bamoun Plateau, Western-Cameroon). *Arab. J. Geosci.* **2019**, *12*, 165. [CrossRef]
32. Pórcel, R.A.D.; Schüth, C.; De León-Gómez, H.; Hoppe, A.; Lehné, R. Land-Use Impact and Nitrate Analysis to Validate DRASTIC Vulnerability Maps Using a GIS Platform of Pablillo River Basin, Linares, N.L., Mexico. *Int. J. Geosci.* **2014**, *5*, 1468–1489. [CrossRef]
33. Singh, S.; Anil, A.G.; Kumar, V.; Kapoor, D.; Subramanian, S.; Singh, J.; Ramamurthy, P.C. Nitrates in the Environment: A Critical Review of Their Distribution, Sensing Techniques, Ecological Effects and Remediation. *Chemosphere* **2022**, *287*, 131996. [CrossRef]
34. Böhlke, J.K. Groundwater Recharge and Agricultural Contamination. *Hydrogeol. J.* **2002**, *10*, 153–179. [CrossRef]
35. DOF Norma Oficial Mexicana NOM-127-SSAI-2021 Agua Para Uso y Consumo Humano.Límites Permisibles de La Calidad Del Agua. 2021. Available online: https://www.dof.gob.mx/nota_detalle.php?codigo=5650705&fecha=02/05/2022#gsc.tab=0. (accessed on 26 June 2023).
36. Gómez, H.; Del Campo, M.; Esteller, M.; Velasco, F.; Alva, E.; Cruz, A. Assessment of Nitrate and Heavy Metal Contamination of Groundwater Using the Heavy Metal Pollution Index: Case Study of Linares, Mexico. *Environ. Earth Sci.* **2020**, *79*, 433. [CrossRef]
37. California Water Boards. Recursos Para Agricultores: Nitrato en el Agua Potable. *Programa Regul. Agric.* **2013**, 1–4.
38. Su, X.; Wang, H.; Zhang, Y. Health Risk Assessment of Nitrate Contamination in Groundwater: A Case Study of an Agricultural Area in Northeast China. *Water Resour. Manag.* **2013**, *27*, 3025–3034. [CrossRef]

39. Ward, M.H. Too Much of a Good Thing? Nitrate from Nitrogen Fertilizers and Cancer. *Rev. Environ. Health* **2009**, *24*, 357–363. [CrossRef]
40. Figueroa-Núñez, A.; Campos-Gaytán, J.R. Simulación Numérica Del Agua Subterránea En El Acuífero Guadalupe, Ensenada, Baja California, México: Caso de Estudio, Condiciones Estacionarias y Transitorias. *Investig. Y Cienc. Univ. Auton. Aguascalientes* **2018**, *75*, 46–54. [CrossRef]
41. CONAGUA. Actualización de La Disponibilidad Media Anual de Agua En El Acuífero Guadalupe (0207). 2015. Available online: https://www.gob.mx/cms/uploads/attachment/file/103407/DR_0207.pdf (accessed on 15 May 2023).
42. CONAGUA. Actualización de La Disponibilidad Media Anual de Agua En El Acuífero Guadalupe (0207). 2020. Available online: https://sigagis.conagua.gob.mx/gas1/Edos_Acuiferos_18/BajaCalifornia/DR_0207.pdf (accessed on 15 May 2023).
43. CONAGUA. Actualización Hidrogeológica Del Acuífero Guadalupe (0207), Estado De Baja California. 2017. Available online: https://sigagis.conagua.gob.mx/gas1/sections/Disponibilidad_Acuiferos.html (accessed on 27 October 2023).
44. Daesslé, L.W.; Mendoza-Espinosa, L.G.; Camacho-Ibar, V.F.; Rozier, W.; Morton, O.; Van Dorst, L.; Lugo-Ibarra, K.C.; Quintanilla-Montoya, A.L.; Rodríguez-Pinal, A. The Hydrogeochemistry of a Heavily Used Aquifer in the Mexican Wine-Producing Guadalupe Valley, Baja California. *Environ. Geol.* **2006**, *51*, 151–159. [CrossRef]
45. Andrade, D.P. Zonificación Hidrogeológica e Hidrogeoquímica Del Acuífero de Valle de Guadalupe, B.C., Universidad Autónoma de Baja California. Master's Thesis, Universidad Autónoma de Baja California, Ensenada Mexico, 2019.
46. Del Toro Guerrero, F.J.; Kretzschmar, T.; Hinojosa Corona, A. Estimacion del Balance Hidrico en Una Cuenca Semiarida, El Mogor, Baja California, México. *Tecnol. Y Ciencias Agua* **2014**, *5*, 69–81.
47. Saiz-Rodríguez, J.A.; Lomeli Banda, M.A.; Salazar-Briones, C.; Ruiz-Gibert, J.M.; Mungaray-Moctezuma, A. Allocation of Groundwater Recharge Zones in a Rural and Semi-Arid Region for Sustainable Water Management: Case Study in Guadalupe Valley, Mexico. *Water* **2019**, *11*, 1586. [CrossRef]
48. Del Toro-Guerrero, F.J.; Vivoni, E.R.; Kretzschmar, T.; Runquist, S.H.B.; Vázquez-González, R. Variations in Soil Water Content, Infiltration and Potential Recharge at Three Sites in a Mediterranean Mountainous Region of Baja California, Mexico. *Water* **2018**, *10*, 1844. [CrossRef]
49. Doerfliger, N.; Jeannin, P.; Zwahlen, F. Water Vulnerability Assessment in Karst Environments: A New Method of Defining Protection Areas Using a Multi-Attribute Approach and GIS Tools (EPIK Method). *Environ. Geol.* **1999**, *39*, 165–176. [CrossRef]
50. Chamanehpour, E.; Sayadi, M.H.; Yousefi, E. The Potential Evaluation of Groundwater Pollution Based on the Intrinsic and the Specific Vulnerability Index. *Groundw. Sustain. Dev.* **2020**, *10*, 100313. [CrossRef]
51. Khosravi, K.; Sartaj, M.; Tsai, F.T.C.; Singh, V.P.; Kazakis, N.; Melesse, A.M.; Prakash, I.; Tien Bui, D.; Pham, B.T. A Comparison Study of DRASTIC Methods with Various Objective Methods for Groundwater Vulnerability Assessment. *Sci. Total Environ.* **2018**, *642*, 1032–1049. [CrossRef]
52. Puerta, R.; Rengifo, J.; Bravo, N. ARCGIS BÁSICO 10, ESRI, Universidad Nacional Agraria De La Selva. 2011. Available online: https://geoinnova.org/libro/manual-de-arcgis-10-basico/ (accessed on 14 February 2022).
53. QGIS Development Team QGIS Desktop 3.22 User Guide. 2022. Available online: https://docs.qgis.org/3.22/pdf/en/QGIS-3.22-DesktopUserGuide-en.pdf (accessed on 16 July 2023).
54. Servicio Geológico Mexicano Carta Geológico-Minera Francisco Zarco I11-D82, Baja California. 2001. Available online: https://www.sgm.gob.mx/GeoInfoMexGobMx/#. (accessed on 28 January 2022).
55. Campos-Gaytan, J.R.; Kretzschmar, T.; Herrera-Oliva, C.S. Future Groundwater Extraction Scenarios for an Aquifer in a Semiarid Environment: Case Study of Guadalupe Valley Aquifer, Baja California, Northwest Mexico. *Environ. Monit. Assess.* **2014**, *186*, 7961–7985. [CrossRef]
56. Esteller, M.; Quentin, E.; Díaz, C. Uso De Sistemas de Información Geográfica (SIG) Para la Determinación de Parámetros Utilizados en La Construcción de Mapas de Vulnerabilidad de Acuíferos. *Rev. Latino-Americana Hidrogeol.* **2002**, *2*, 17–30.
57. Thermo Fisher Scientific Inc. *Thermo Scientific Dionex Aquion Ion Chromatography System Operator's Manual*; Thermo Fisher Scientific Inc.: Munich, Germany, 2016; pp. 1–3. Available online: https://assets.thermofisher.com/TFS-Assets/CMD/manuals/man-22176-97006-aquion-rfic-man2217697006-en.pdf (accessed on 14 March 2022).
58. Kurczyn-Robledo, J.A.; Kretzschmar, T.; Hinojosa-Corona, A. Evaluación del Escurrimiento Superficial en el Noreste del Valle de Guadalupe, B.C., México, Usando el Método de Curvas Numeradas y Datos de Satélite. *Rev. Mex. Cienc. Geol.* **2007**, *24*, 1–14.
59. Umar, M.; Khan, S.N.; Arshad, A.; Aslam, R.A.; Khan, H.M.S.; Rashid, H.; Pham, Q.B.; Nasir, A.; Noor, R.; Khedher, K.M.; et al. A Modified Approach to Quantify Aquifer Vulnerability to Pollution towards Sustainable Groundwater Management in Irrigated Indus Basin. *Environ. Sci. Pollut. Res.* **2022**, *29*, 27257–27278. [CrossRef] [PubMed]
60. Manjarrez-Domínguez, C.; Uc-Campos, M.I.; Esparza-Vela, M.E.; Baray-Guerrero, M.D.R.; Giner-Chávez, O.; Santellano-Estrada, E. Geospatial-Temporal Dynamics of Land Use in the Juárez Valley: Urbanization and Displacement of Agriculture. *Sustainability* **2023**, *15*, 8499. [CrossRef]

Disclaimer/Publisher's Note: The statements, opinions and data contained in all publications are solely those of the individual author(s) and contributor(s) and not of MDPI and/or the editor(s). MDPI and/or the editor(s) disclaim responsibility for any injury to people or property resulting from any ideas, methods, instructions or products referred to in the content.